Preprints (www.preprints.org) | NOT PEER-REVIEWED | Posted: 8 June 2022 doi:10.20944/preprints202206.0109.v1

Article

An Advanced Approach for Mgznal-LDH Catalysts Synthesis Used in Claisen-Schmidt Condensation

Rodica Zăvoianu [1,2], Silvana-Denisa Mihăilă [1,2], Bogdan Cojocaru [1,2], Mădălina Tudorache [1,2], Vasile I. Parvulescu [1,2], Octavian Dumitru Pavel [1,2]*, Solon Oikonomopoulos [3] and Elisabeth Egholm Jacobsen [3,*]

[1] University of Bucharest, Faculty of Chemistry, 4-12 Regina Elisabeta Av., Bucharest, 030018, Romania
[2] Research Center for Catalysts & Catalytic Processes, Faculty of Chemistry, University of Bucharest, 4-12, Blv. Regina Elisabeta, 030018 Bucharest, Romania
rodica.zavoianu@chimie.unibuc.ro (R.Z.); silvana.mihaila@s.unibuc.ro (S.D.M.); bogdan.cojocaru@chimie.unibuc.ro (B.C.); madalina.sandulescu@g.unibuc.ro (M.S.); vasile.parvulescu@chimie.unibuc.ro (V.I.P.); octavian.pavel@chimie.unibuc.ro (O.D.P.)
[3] Norwegian University of Science and Technology, Department of Chemistry, Høgskoleringen 5, 7491 Trondheim, Norway
solon.oikonomopoulos@ntnu.no (S.O.); elisabeth.e.jacobsen@ntnu.no (E.E.J.)
* Correspondence: octavian.pavel@chimie.unibuc.ro (O.D.P.) and elisabeth.e.jacobsen@ntnu.no (E.E.J.); Tel.: +40213051464 and +4798843559

Abstract: Using of the organic base tetramethylammonium hydroxides (TMAH) is a viable, cheap and fast route, for the MgZnAl-LDH type materials synthesis by both co-precipitation and mechano-chemical methods. TMAH provided several advantages as smaller quantity of water required in the washing step compared to the use of inorganic alkalis, prevention of LDH contamination with alkali cations, acting as template molecule in texture tailoring along with disadvantages as its presence in small quantities in the resulting layered materials. Regardless the use of organic / inorganic bases and co-precipitation / mechano-chemical methods, zincite stable phase was found in all the synthesized solids. The basicity of catalysts followed the trend: mixed oxides > reconstructed > parent LDH. The memory effect of LDH is supported only by the presence of Mg and Al cations, while Zn remains as zincite stable phase. The catalytic activities for Claisen-Schmidt condensation of benzaldehyde with cyclohexanone provided values higher than 90% after 2h, with a total selectivity in 2,6-dibenzylidenecyclohexanone, while in self-condensation of cyclohexanone no more than 7.29% after 5h. These behaviors depended on catalysts basicity as well as the planar rigidity of the compound.

Keywords: Layered Double Hydroxides (LDH); mechano-chemical / co-precipitation synthesis; organic alkalis (tetramethylammonium hydroxides); memory effect; Claisen-Schmidt condensation; self-cyclohexanone condensation

1. Introduction

Recently, a remarkable increase of the layered double hydroxides (LDH) utilization in various domains such as catalysts for fine chemicals syntheses [1-4], adsorbents for environmental protection [5-7], corrosion inhibitors [8], polymer additives [9], drug delivery [10], building materials [11], battery manufacture [12,13], etc. These materials have a general formula $\mathbf{[M^{2+}_{1-x}M^{3+}_{x}(OH)_2]^{x+}[A^{n-}_{x/n}]\cdot mH_2O}$ [4], where $\mathbf{M^{2+}}$ and $\mathbf{M^{3+}}$ are bi- and trivalent cations adopting an octahedral geometry [14], **A** is an anions with charge **n**, **x** is equal to the ratio $M^{3+}/(M^{2+}+M^{3+})$ and **m** is the number of water molecules. This formula is not restricted only to compositions with two different cations, but with multiple types of bivalent and trivalent cations which may generate ternary or quaternary compounds [15,16]. A specific property of these materials is the so-called *memory effect* that allows the reconstruction of the layered structure by hydrating the mixed oxides obtained from thermal treatments up to 500-600 °C of the parent LDH [4]. This reconstruction of the layered struc-

© 2022 by the author(s). Distributed under a Creative Commons CC BY license.

Preprints (www.preprints.org) | NOT PEER-REVIEWED | Posted: 8 June 2022 doi:10.20944/preprints202206.0109.v1

ture is carried out by two mechanisms: *i)* a dissolution – re-crystallization mechanism suggested by Ulibarri and Takehira [17,18] and *ii)* retro – topotactic transformation proposed by Marchi and Apesteguía [19]. Besides the fact that a specific basicity can be afforded by the partial replacement of the interlayer carbonate anions with some pronounced basic ones [20], *i.e.* hydroxyl groups, it is also possible to insert in the layered structure anions with large dimensions [21]. Traditionally, the layered catalytic materials are obtained by several methods [22] such as: co-precipitation (at low or high supersaturation, urea hydrolysis), ion-exchange, rehydration using structural memory effect, hydrothermal, secondary intercalation, etc. Other methods which include the mechano-chemical synthesis [23], the exfoliation in aqueous solution [24], the dry exfoliation [25], or the electrochemical synthesis [26], were developed recently aiming to replace the usual ones, etc. However, most traditional methods use inorganic alkalis (*i.e.* NaOH, KOH, Na_2CO_3, K_2CO_3 etc.), that can often lead to LDH contamination with traces of alkaline metals cations (*e.g. ppm* or *ppb* levels). Besides these, a large amount of energy, water (in the washing step) or the uses of specific glassware for the preparation are other disadvantages that these inorganic alkalis generate. A new approach that removes all these drawbacks considers the use of organic alkalis for LDH synthesis [27-29]. However, the replacement of inorganic alkalis with organic ones could be somehow restrictive due to their price, inadequate solubility in water, their possibility to decompose during preparation or storage over time as well as the possible presence of impurities in their composition, etc. However, all these issues can be avoided by proper organic alkali choosing and manipulation under optimal conditions.

Among the possible utilizations of LDHs, an important one is their use as catalysts for fine chemicals synthesis. Since 1880 when Schmidt [30] reported for the first time the aldol condensation between furfural and acetaldehyde / acetone, being developed by Claisen [31], the aldol condensation become one of the most important reactions in organic chemistry, where a C—C bond is generated in the presence of some catalysts with acid / base character [3]. A special case of Claisen-Schmidt condensation is the reaction between benzaldehyde and cyclohexanone which generated two valuable compounds for fine chemistry and not only, *i.e.* 2-benzylidenecyclohexanone (2-BCHO) [32] and 2,6-dibenzylidenecyclohexanone (2,6-DBCHO) [33], respectively. To date is still under debate, which are the parameters responsible for selecting a direction towards mono- or di-condensation products. Until now, Tang [34] and Sluban [35] obtained a high yield of 96% for the mono-condensation product 2-BCHO in the presence of modified CaO with benzyl bromide and HTiNTs. Meanwhile, there are numerous publications reporting higher yields for the di-condensation product (2,6-DBCHO). Thus, an activated fly ash catalyst [36], generated 56% yield; a grinded solid NaOH leads to 2,6-DBCHO yields over 96% [37]; NaP Zeolite/$CoFe_2O_4$/Am-Py (1:4) catalyst in free solvent condition [38] yields 92% 2,6-DBCHO ; using quaternary ammonium surfactants with *n*-hexadecyl group micellar system (C_{16}QAS) as catalyst [39] a yield of 73.8% for 2,6-DBCHO; while $SOCl_2$, in anhydrous ethanol ($SOCl_2$/EtOH) [40] yielded more than 92%, .

Nevertheless, during the Claisen-Schmidt condensation two secondary reactions may occur [3], *i.e.* the cyclohexanone self-condensation to 2-(1-cyclohexenyl)-cyclohexanone (2-CyCHO) and 2,6-dicyclohexylidencyclohexanone (2,6-DCyCHO) compounds in the presence of catalytic base sites, as well as the oxidation of benzaldehyde to benzoic acid, especially since it is known that this reaction takes place non-catalytically under ambient conditions in air presence.

Given the above, this paper aims to bring new insights on the influence of the synthesis methods (traditional co-precipitation / non-traditional mechanical-chemical) as well as that of the alkalis used (traditional inorganic / non-traditional organic) in tailoring the physico-chemical properties of MgZn/Al LDH. Also, the optimum activity of LDH-type materials, mixed oxides and reconstructed LDH, in the Claisen-Schmidt condensation between benzaldehyde and cyclohexanone and in the cyclohexanone self-condensation will be highlighted.

Preprints (www.preprints.org) | NOT PEER-REVIEWED | Posted: 8 June 2022 doi:10.20944/preprints202206.0109.v1

2. Results and Discussion

2.1. Characterization of Catalysts

The XRD pattern for the LDH synthesized through a traditional route by co-precipitations in the presence of inorganic alkalis, LDH-MgZnAl-CO_3^{2-}/OH^--CP, presents sharp and symmetric reflections at small angles for (003), (006), (009), (012), (015), (018) planes, while at higher one, broad and weak reflections for (110) and (113) planes, which are representative for LDH type materials (ICDD 70-2151), Figure 1A [23].

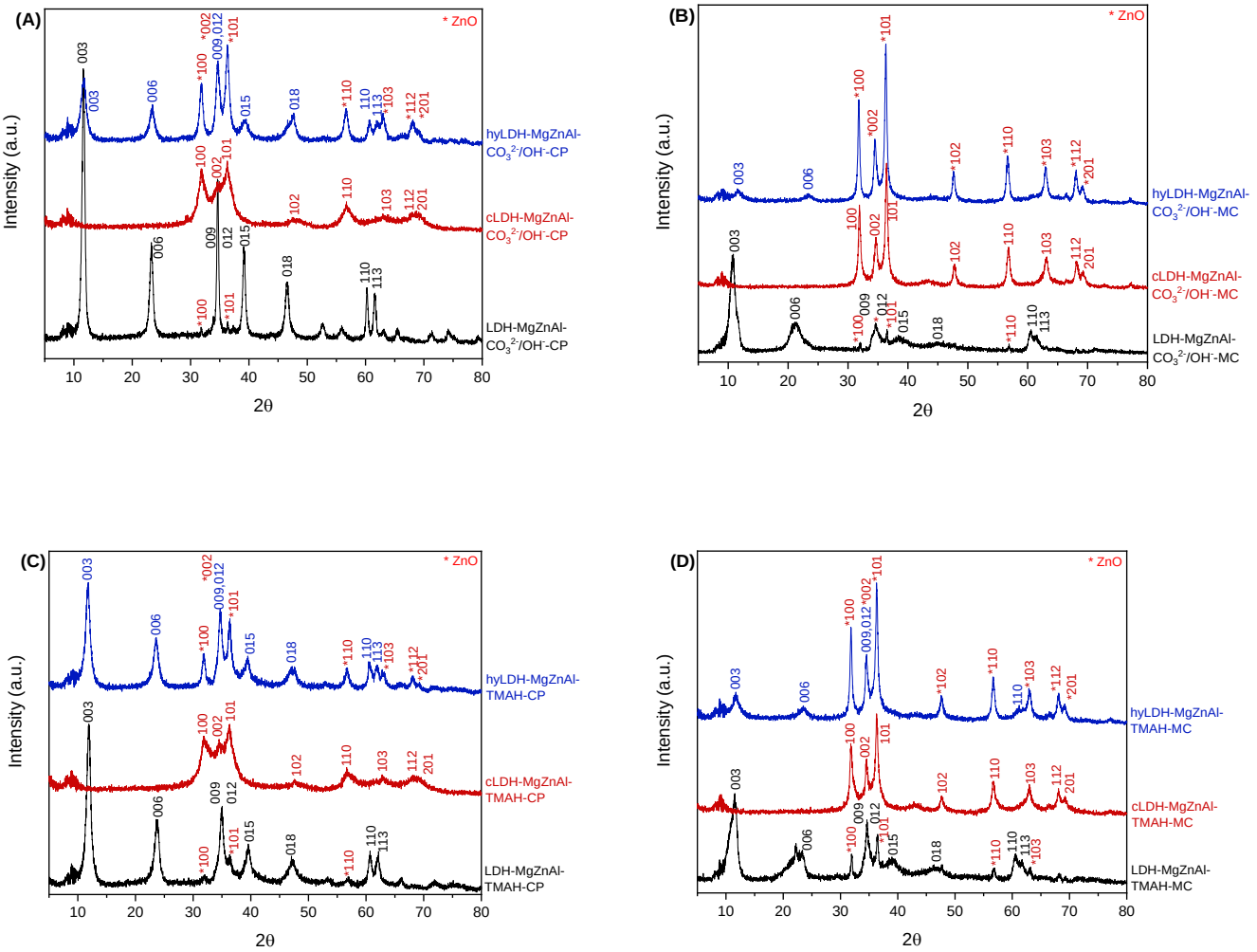

Figure 1. XRD patterns of the materials synthesized though (A) co-precipitation and (B) mechanochemical, both in the presence of Na_2CO_3/NaOH as well as (C) co-precipitation and (D) mechanochemical, both in the presence of TMAH.

These reflections are indexed in a hexagonal lattice with an *R3m* rhombohedral symmetry. Aside from those, some additional fine diffraction lines corresponding to zincite phase are appearing in the domain of 2θ=31-38° (ICDD 005-0664). Its presence is noticeable in the XRD pattern of the calcined material, cLDH-MgZnAl-CO_3^{2-}/OH^--CP, where diffraction lines corresponding to ZnO ((100), (002) and (101)) are more intense. Reconstruction by memory effect leads to a mixture of stable zincite phase and Mg/Al LDH. In the same time the IFS parameter (*i.e.* the interlayer distance) decreases from 2.82 Å to 2.80 Å and $2\theta_{003}$ also shifts towards a higher value from 11.6259° to 11.6421°, Table 1, thus noting the presence of smaller species in the interlayer space which, according to the literature

Preprints (www.preprints.org) | NOT PEER-REVIEWED | Posted: 8 June 2022 doi:10.20944/preprints202206.0109.v1

[20], are OH^- groups that partially replace the CO_3^{2-} groups following the calcination-reconstruction process, behavior observed as well in DRIFT spectra, Figure 2.

Table 1. The network parameter of samples.

Hydrotalcite samples	Lattice parameters		IFS* (Å)	$2\theta_{003}$ (°)	I_{003}/I_{006}	I_{003}/I_{110}	$FWHM_{003}$	D** (Å)
	a (Å)	***c*** (Å)						
LDH-MgZnAl-CO_3^{2-}/OH^--CP	3.0717	22.8689	2.82	11.6259	2.96	5.54	0.6064	131.8
hyLDH-MgZnAl-CO_3^{2-}/OH^--CP	3.0497	22.8017	2.80	11.6421	1.97	3.42	1.1043	72.4
LDH-MgZnAl-CO_3^{2-}/OH^--MC	3.0504	22.4314	2.68	11.8652	2.54	5.33	0.8885	90.0
hyLDH-MgZnAl-CO_3^{2-}/OH^--MC	3.0497	22.6427	2.75	11.7234	2.20	4.48	0.9709	82.3
LDH-MgZnAl-TMAH-CP	3.0617	24.7662	3.46	10.8279	3.57	5.08	1.1644	68.6
hyLDH-MgZnAl-TMAH-CP	2.9757	22.7965	2.80	11.6610	1.59	1.13	0.9020	88.6
LDH-MgZnAl-TMAH-MC	3.0580	23.6969	3.10	11.3150	2.83	3.45	1.6050	49.8
hyLDH-MgZnAl-TMAH-MC	3.0535	22.7515	2.78	11.6700	2.18	3.45	1.1800	67.7
Mixed oxides samples	***a*** (Å)			$2\theta_{101}$ (°)	I_{003}		$FWHM_{101}$	D*** (Å)
cLDH-MgZnAl-CO_3^{2-}/OH^--CP	4.9536			36.2400	279		1.8266	45.8
cLDH-MgZnAl-CO_3^{2-}/OH^--MC	4.9483			36.3628	257		1.5500	53.9
cLDH-MgZnAl-TMAH-CP	4.9332			36.3949	736		0.4925	169.9
cLDH-MgZnAl-TMAH-MC	4.9449			36.3055	175		0.6023	138.9

*IFS represents the interlayer free distance; 4.8Å brucite sheet thickness [41].
**D represents the mean crystallite size (derived from the Debye–Scherrer equation) determined from the FWHM of the (003) reflection for LDH samples.
***D represents the mean crystallite size (derived from the Debye–Scherrer equation) determined from the FWHM of the (101) reflection for mixed oxides.

The easily noticeable decrease of ***a*** network parameter (*i.e.* the distance between the network cations) is due to the extraction of Zn from the LDH network followed by the stable phase of zincite synthesis made by calcination. The mechanochemically LDH, LDH-MgZnAl-CO_3^{2-}/OH^--MC, present similar particularities to the above-mentioned, Figure 1B, but the amount of zincite increases and that of LDH phase decreased. Moreover, the number of interlayer species with small size, *i.e.* OH^-, is higher compared to LDH obtained by co-precipitation, a fact highlighted by an IFS value of 2.68Å compared to 2.82Å and a shifting from $2\theta_{003}$ to 11.8652°. After the reconstruction of the layered structure, hyLDH-MgZnAl-CO_3^{2-}/OH^--MC, a large amount of zincite remained as the stable phase. This behavior simultaneously leads to an increase in the IFS value of 2.75Å as well as a shift to lower values of 11.7234 for $2\theta_{003}$. The mean crystallite size derived from the Debye-Scherrer equation shows an insignificant variation (from 90.0Å to 82.3Å) compared to the one noticed for co-precipitated materials (from 131.8Å to 72.4Å). The use of TMAH in LDH synthesis by both co-precipitation and mechano-chemical methods produced pure LDH structure mixed with small amounts of zincite phase, Figure 1C,D. The IFS values of LDH obtained by both methods are increased (LDH-MgZnAl-TMAH-CP of 3.46Å and LDH-MgZnAl-TMAH-MC of 3.10Å) because, besides OH^- and CO_3^{2-} groups, in the interlayer space there are also small amounts of TMAH as well as tri-methyl amine (an ubiquitous impurity from TMAH; its existence being also demonstrated by DRIFT). The calcination processes eliminate both organic compounds as dimethyl ether and methanol [42]. The LDH structure reconstruction by the memory effect is present for all materials synthesized in TMAH presence. The diffraction lines of hyLDH-MgZnAl-TMAH-CP and hyLDH-MgZnAl-TMAH-MC are more intense compared to those of the materials synthesized with inorganic alkalis. All mixed oxides samples prepared by calcination of parent LDH show only ZnO lines with no important differences in ***a*** network parameter and $2\theta_{101}$, excepting of the mean crystallite size where organic alkalis generated values 3 times

Preprints (www.preprints.org) | NOT PEER-REVIEWED | Posted: 8 June 2022 doi:10.20944/preprints202206.0109.v1

higher compared with the inorganic one, Table 1. Because the diffraction lines corresponding to the Mg(Al^{3+})O solid solution of MgO-periclase type (JCPDS-45-0946) phases are not obvious, this phase is highly dispersed.

DRIFT spectra of the investigated LDH, Figure 2A,B,C,D, present a large band in the 3700-3400 cm^{-1} domain corresponding to the vibration of hydroxyl groups, υ_{O-H}, that at 3000 cm^{-1} is assigned to hydrogen bonds between carbonate anion and water molecules, both situated in the interlayer space [43], a band at 1638-1650 cm^{-1} characteristic to the H_2O bending vibration of interlayer LDH structure, a band at 1200-600 cm^{-1} assigned to the CO_3^{2-} group vibration, while below 600 cm^{-1} of Mg–O, Zn–O and Al–O bonds.

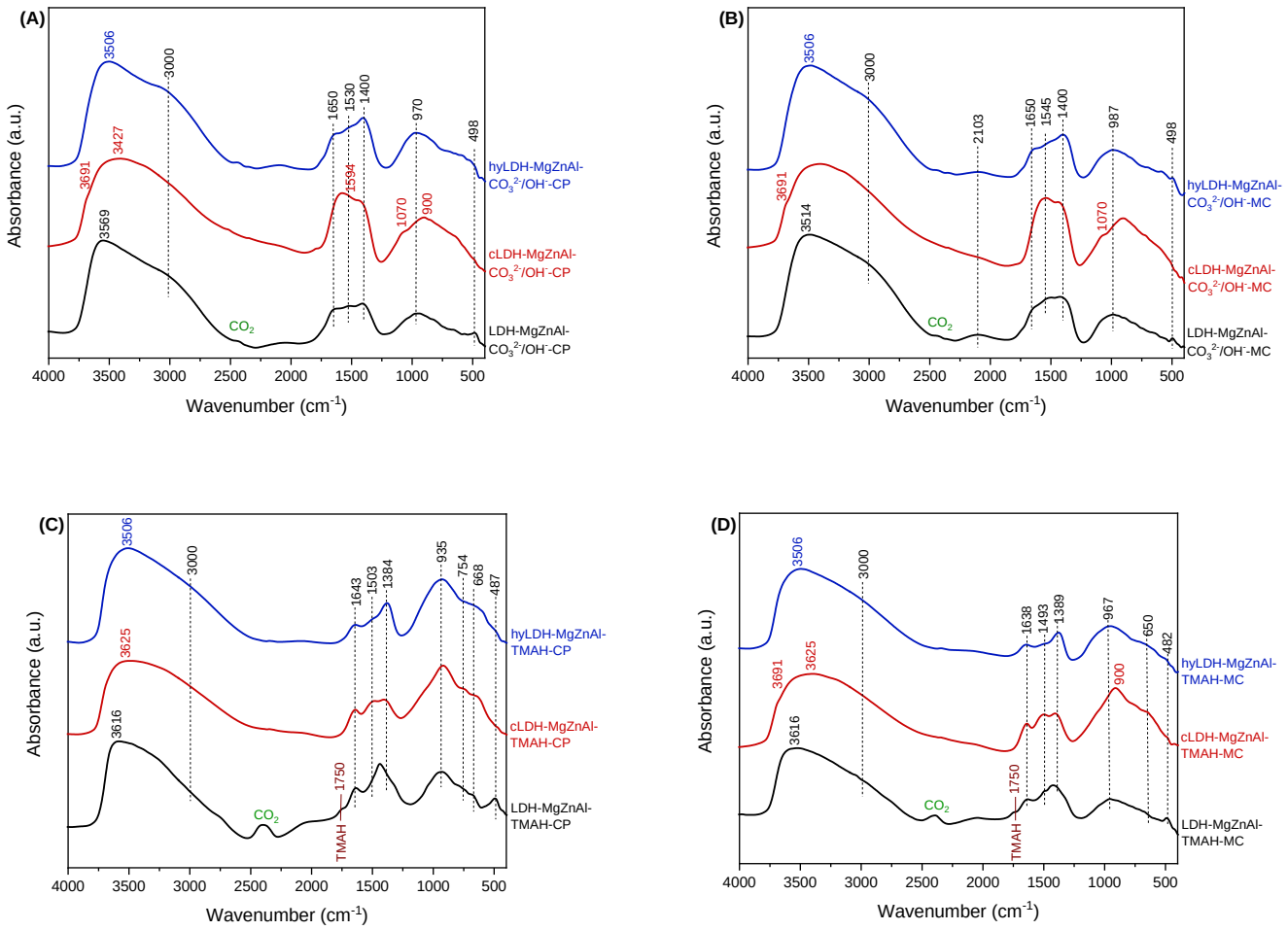

Figure 2. DRIFT spectra of the materials synthesized though (A) co-precipitation and (B) mechanochemical, both in the presence of Na_2CO_3/NaOH as well as (C) co-precipitation and (D) mechanochemical, both in the presence of TMAH.

The band at 1750 cm^{-1} for samples synthesized with TMAH is assigned to this hydrolysis agent, which is present in small quantities in the pores of LDH. This remnant compound, due to its pronounced base character, generated a higher physisorption of atmospheric CO_2 exhibiting a band at 2450 cm^{-1} (stronger than that appearing in the spectra of materials prepared with inorganic alkalis). Noteworthy in the case of TMAH prepared samples, the bands from 1650 cm^{-1} and 1400 cm^{-1} shifted to 1640-1638 cm^{-1} and 1389-1384 cm^{-1}, respectively. The calcination at 460 °C eliminates the remnant TMAH and adsorbed CO_2, leading to the total disappearing of their corresponding IR adsorption bands. Besides that there is also a partial removal of OH^- and CO_3^{2-} from the network leading to a decreased intensity of the corresponding bands. However, bands assigned to the carbonate anions persisted till the calcination at temperatures of 650 - 700 °C, when stable oxides are

Preprints (www.preprints.org) | NOT PEER-REVIEWED | Posted: 8 June 2022 doi:10.20944/preprints202206.0109.v1

obtained, and the memory effect is lost [19]. The spectra of the calcined samples present also a band characteristic stretching vibrations of structural hydroxyl groups which are coordinated to Mg or Al octahedral at 3691 cm^{-1} [44]. This phase is highly dispersed in the solid matrix since its reflections are absent in the XRD patterns. The bands at 3000 cm^{-1} and that at 1638-1650 cm^{-1} are well restored in the spectra of the reconstructed samples. Simultaneously, the band at 1400-1384 cm^{-1} becomes stronger. The UV-VIS spectra of the samples obtained in the presence of inorganic alkalis using both preparation methods, Figure 3A,B, show a large absorption band in the wavelength range of 240-380 nm with maxima at 348 nm and 359 nm for the LDH. This shifting is due to the presence of zincite phase in higher amount for samples obtained through mechano-chemical method. In mixed oxides samples, the maxima identified at 363 nm and 366 nm are corresponding to zinc oxide nanoparticles as impurities in the materials [45], while the ones at 289 nm and 281 nm are attributed to the band gap absorption in ZnO/MgO nanocomposites that present larger band gaps as compared to ZnO [46]. The bands at 212 and 215 nm indicated the presence of $Mg(OH)_2$ and MgO [47]. For samples obtained in the presence of TMAH by both routes, Figure 3C,D, the common band at 210 nm indicates the presence of the organic base in their structure, while the ones at 313 nm and 315 nm are due to the presence of zincite phase inside of the layered structure. Mixed oxides and reconstructed LDH also show bands for zincite phase shifted to higher values for layered materials.

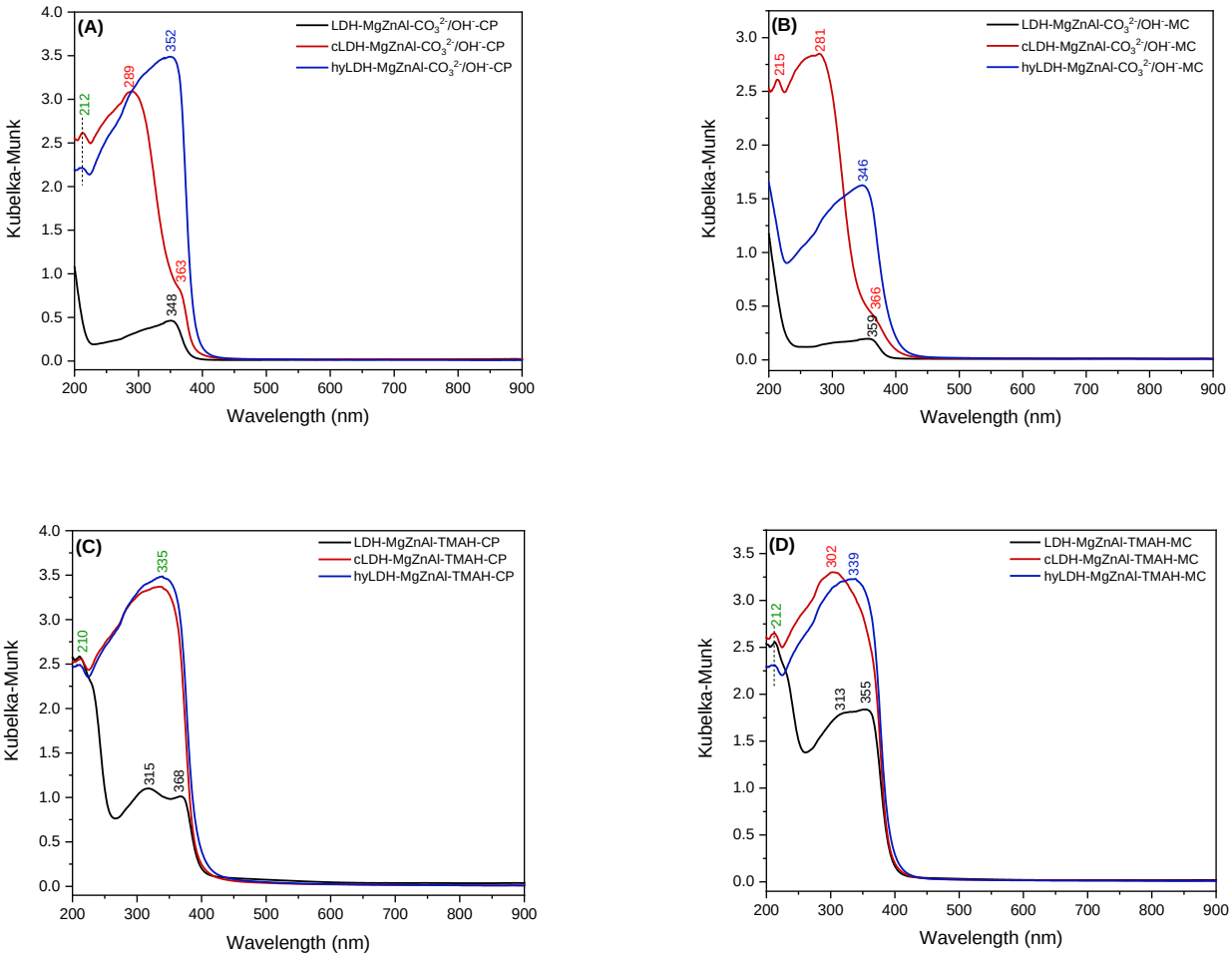

Figure 3. UV-Vis spectra of the materials synthesized though (A) co-precipitation and (B) mechano-chemical, both in the presence of Na_2CO_3/NaOH as well as (C) co-precipitation and (D) mechano-chemical, both in the presence of TMAH.

Preprints (www.preprints.org) | NOT PEER-REVIEWED | Posted: 8 June 2022 doi:10.20944/preprints202206.0109.v1

The basicity of samples, Table 2, decreased in the order mixed oxides > reconstructed LDH > parent LDH samples, trend valid for both strong base sites as well as sum of weak and medium base sites, regardless the synthesis route. However, there was a slight increase in the basicity for the samples prepared by mechano-chemical route. Also, the presence of small TMAH in LDH provided a pronounced base character compared to the LDH prepared with inorganic alkalis. In the meantime, the reconstructed LDH show a decreased specific surface area comparative to those of parent ones due to the tendency of hexagonal lamellar crystals to cluster together in large conglomerates system, under vermiculate form, involving less defined platelets which affect the accessibility of reactants as well as probe molecule as N_2 toward active sites [48,49]. However, the partial replacement of carbonate anions with hydroxyl groups following calcination-hydration process leads to an increase in the basicity of the reconstructed samples due to the pronounced base character of these groups, Table 2. Regarding the textural properties of mixed oxides, they are in the proper range of these types of materials [4].

Table 2. The surface area and basicity of materials.

Hydrotalcite samples	Surface area ($m^2 \cdot g^{-1}$)	Pore volume ($cm^3 \cdot g^{-1}$)	Average pore width (Å)	Total number of base sites ($mmol \cdot g^{-1}$)*	Distribution of base sites	
					Strong base sites ($mmol \cdot g^{-1}$)**	Weak and medium base sites ($mmol \cdot g^{-1}$)***
LDH-MgZnAl-CO_3^{2-}/OH^--CP	69	0.387	222	7.23	0.48	6.75
cLDH-MgZnAl-CO_3^{2-}/OH^--CP	258	0.843	124	10.38	0.53	9.85
hyLDH-MgZnAl-CO_3^{2-}/OH^--CP	25	0.186	238	8.93	0.57	8.36
LDH-MgZnAl-CO_3^{2-}/OH^--MC	150	0.498	132	7.42	0.51	6.91
cLDH-MgZnAl-CO_3^{2-}/OH^--MC	266	0.845	121	10.48	0.57	9.91
hyLDH-MgZnAl-CO_3^{2-}/OH^--MC	28	0.203	208	8.99	0.61	8.38
LDH-MgZnAl-TMAH-CP	2	0.005	115	7.71	0.50	7.21
cLDH-MgZnAl-TMAH-CP	235	0.765	112	10.64	0.55	10.09
hyLDH-MgZnAl-TMAH-CP	1	0.004	118	9.36	0.59	8.77
LDH-MgZnAl-TMAH-MC	44	0.118	106	7.85	0.54	7.31
cLDH-MgZnAl-TMAH-MC	241	0.798	124	10.66	0.56	10.10
hyLDH-MgZnAl-TMAH-MC	9	0.104	118	9.40	0.64	8.76

*mmol of acrylic acid.
**mmol of phenol.
***the difference between total number of base sites - strong base sites.

The used of TMAH as organic alkali in synthesis of LDH, by both co-precipitation and mechano-chemical methods, act also as template molecule, Figure 4. The mechano-chemical method compared to the co-precipitation one in the presence of traditional inorganic alkali leads to different pore widths (*i.e.* with maxima at 37Å, 81Å, 190Å and 283Å, respectively). While preparation with traditional inorganic alkali leads to a large pore width with maxima of 426Å for LDH-MgZnAl-CO_3^{2-}/OH^--CP and 283Å for LDH-MgZnAl-CO_3^{2-}/OH^--MC, respectively, the preparation in the presence of organic alkali tends to decrease the pore width leading to two well defined maxima in Figure 4 C,D: one at 36Å for LDH-MgZnAl-TMAH-CP and 33Å for LDH-MgZnAl-TMAH-MC, and the second one at 199Å for LDH-MgZnAl-TMAH-CP and 120Å for LDH-MgZnAl-TMAH-MC. The appearance of these two domains is not strange because the porosity is due to the size of the organic compounds, tri-methyl amine for the lower value and TMAH for the higher one.

Preprints (www.preprints.org) | NOT PEER-REVIEWED | Posted: 8 June 2022 doi:10.20944/preprints202206.0109.v1

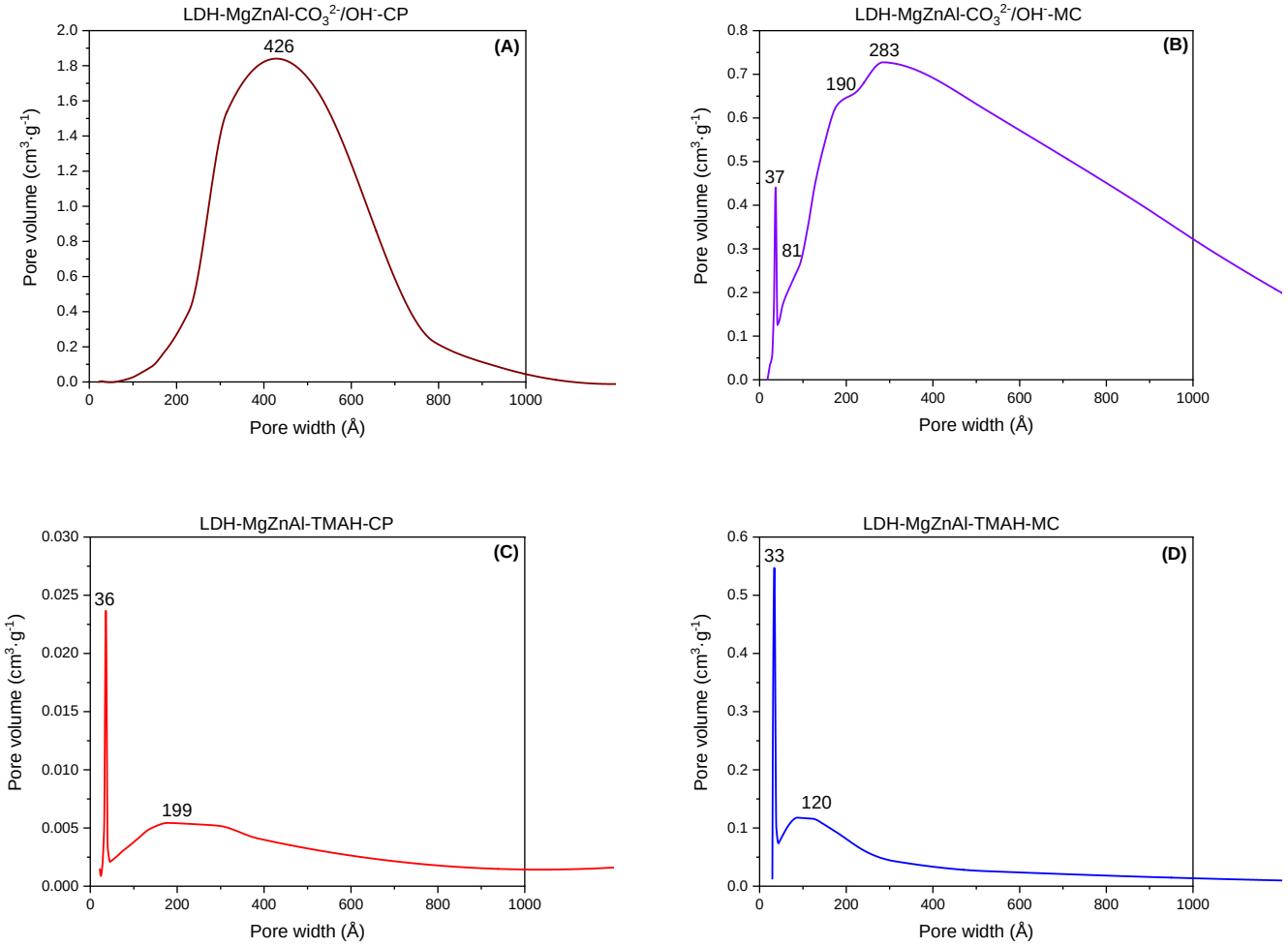

Figure 4. The representation of LDH sample pore widths.

2.2. Catalytic Activity

2.2.1. Claisen-Schmidt condensation

The blank test at room temperature after 5h is in the range of experimental errors of 0.97% in cyclohexanone conversion, increasing at 9.13% at 120 °C and 2h, with total selectivity in 2,6-DBCHO. The cyclohexanone conversion followed the same order: mixed oxides > reconstructed LDH > parent LDH samples, regardless the preparation method, with total selectivity to 2,6-DBCHO, Figure 5. Also, there is an improvement in the catalytic activities of materials prepared in the presence of organic alkalis compared to those prepared with inorganic alkalis, regardless of the preparation methods. However, a linear dependence between total basicity and conversion values was determined, Figure 6. Noteworthy, at the end of the reactions, no products from self-cyclohexanone condensations or benzoic acid have been found in the analyzed reaction mixtures. The total selectivity towards 2,6-DBCHO is also explained by the possibility of 2-BCHO to adsorb onto active sites from pores, with no steric hindrance due to the non-planar shape of this molecule. In the same note, the presence of zincite phase into a different extent may also play a role in increasing the yield to 2,6-DBCHO. The lower activity was noticed for the samples prepared with inorganic alkalis by mechano-chemical method. The comparison of the methods types as well as of the hydrolysis agents used reveals the benefits presented by the use of organic alkalis instead of inorganic ones but also of the co-precipitation method over the mechano-chemical one.

Preprints (www.preprints.org) | NOT PEER-REVIEWED | Posted: 8 June 2022 doi:10.20944/preprints202206.0109.v1

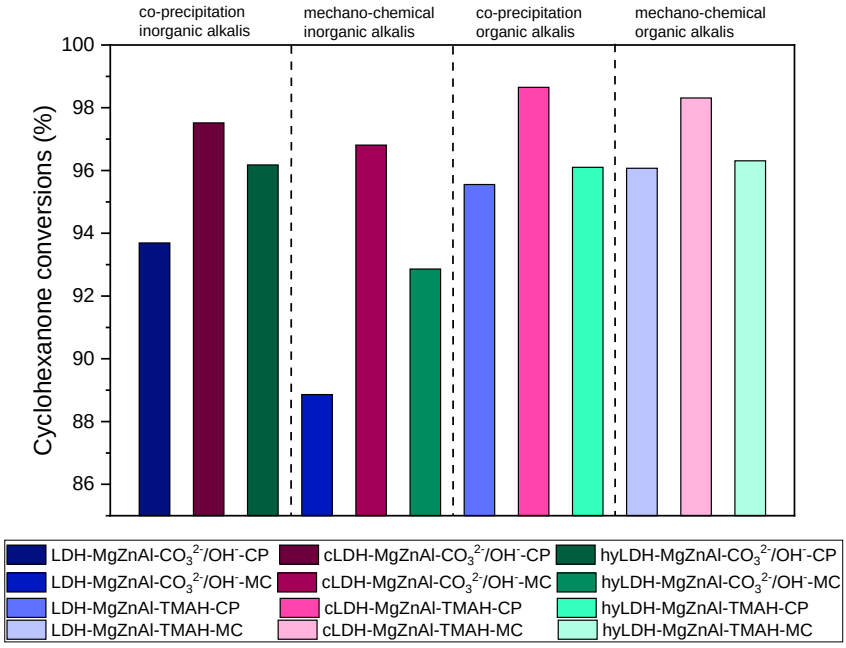

Figure 5. Cyclohexanone conversion after aldol condensation for 2 h, 120 °C, 20 mg of catalyst.

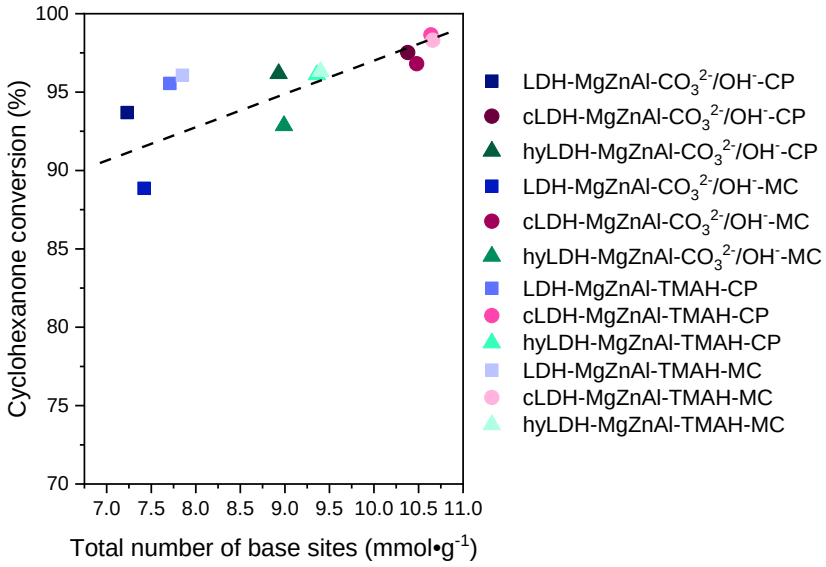

Figure 6. The cyclohexanone conversion *vs.* total number of base sites for investigated catalysts.

2.2.2. Cyclohexanone self-condensation

Blank reaction at room temperature or reflux after 5h did not provided more than 0.19% of cyclohexanone conversion. The cyclohexanone conversions are significantly lower than those reached in Claisen-Schmidt condensation and their magnitude follows the same variation trend: mixed oxides > reconstructed LDH > parent LDH samples, regardless the preparation method. There is also a high selectivity to the mono-condensed product, Table 3.

Preprints (www.preprints.org) | NOT PEER-REVIEWED | Posted: 8 June 2022 doi:10.20944/preprints202206.0109.v1

This changing in paradigm compared to that presented for Claisen-Schmidt condensation, where the selectivity was total to the *di*-condensate compound, is due to the rigidity of the double bond connecting cyclohexane moieties in the *mono*-condensate compound, which leads to steric hindrances in accessing the porous structure of the catalyst. This fact is confirmed also by the dependence of cyclohexanone conversion *vs.* total number of base sites Figure 7.

Table 3. Experimental data gathered for cyclohexanone conversion after 5 h, reflux, 5 %wt. catalyst, solvent-free.

Catalysts	Conv. $C_6H_{10}O$ (%)	Sel. A (%)	Sel. A1 (%)	Sel. B (%)	Sel. B1 (%)
LDH-MgZnAl-CO_3^{2-}/OH^--CP	1.01	69.00	27.31	1.93	1.76
cLDH-MgZnAl-CO_3^{2-}/OH^--CP	1.09	75.31	24.31	0.22	0.16
hyLDH-MgZnAl-CO_3^{2-}/OH^--CP	0.70	69.74	29.64	0.44	0.17
LDH-MgZnAl-CO_3^{2-}/OH^--MC	0.45	66.39	33.61	0.00	0.00
cLDH-MgZnAl-CO_3^{2-}/OH^--MC	0.80	73.74	26.26	0.00	0.00
hyLDH-MgZnAl-CO_3^{2-}/OH^--MC	0.49	69.87	30.13	0.00	0.00
LDH-MgZnAl-TMAH-CP	2.65	73.35	11.36	8.32	6.97
cLDH-MgZnAl-TMAH-CP	7.29	82.48	15.08	1.70	0.74
hyLDH-MgZnAl-TMAH-CP	6.23	75.73	12.20	1.53	0.55
LDH-MgZnAl-TMAH-MC	0.78	76.82	19.75	1.98	1.45
cLDH-MgZnAl-TMAH-MC	1.03	80.30	19.70	0.00	0.00
hyLDH-MgZnAl-TMAH-MC	0.67	74.21	25.79	0.00	0.00

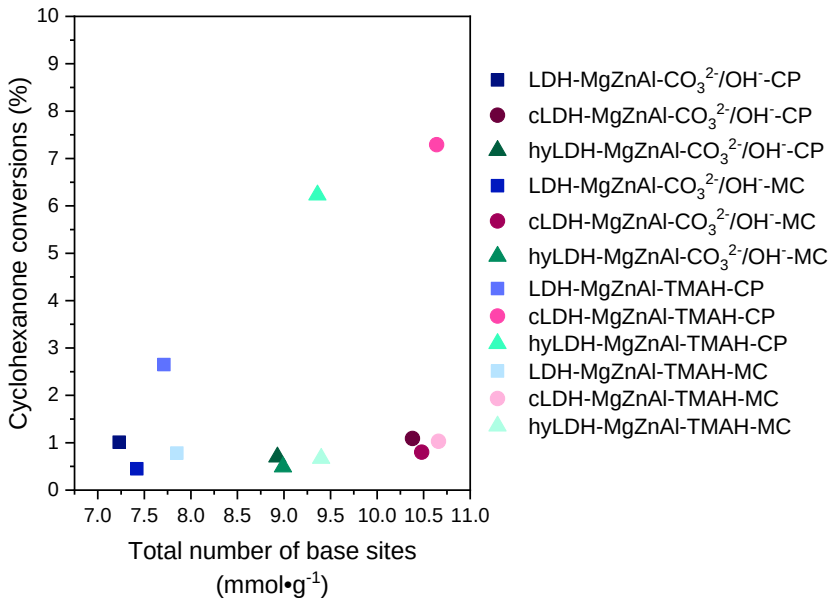

Figure 7. Cyclohexanone conversion *vs.* total number of base sites of investigated catalysts in self-cyclohexanone condensation.

Preprints (www.preprints.org) | NOT PEER-REVIEWED | Posted: 8 June 2022 doi:10.20944/preprints202206.0109.v1

The selectivities in the *di*-condensation product do not exceed 10% since their occurrence is related only to the active sites on the external surface of the solid catalysts. Therefore, the best catalytic activities are presented by the materials obtained in the presence of organic alkalis and the co-precipitation method.

2.2. Catalyst reusability

The stability of catalysts (LDH-MgZnAl-TMAH-CP, cLDH-MgZnAl-TMAH-CP and hyLDH-MgZnAl-TMAH-CP) was checked in three consecutive Claisen-Schmidt condensation runs. After that, the conversion decreased with less than 4% and no modification of diffraction lines in XRD patterns thus confirming the stability of these materials in this reaction, Figure 8.

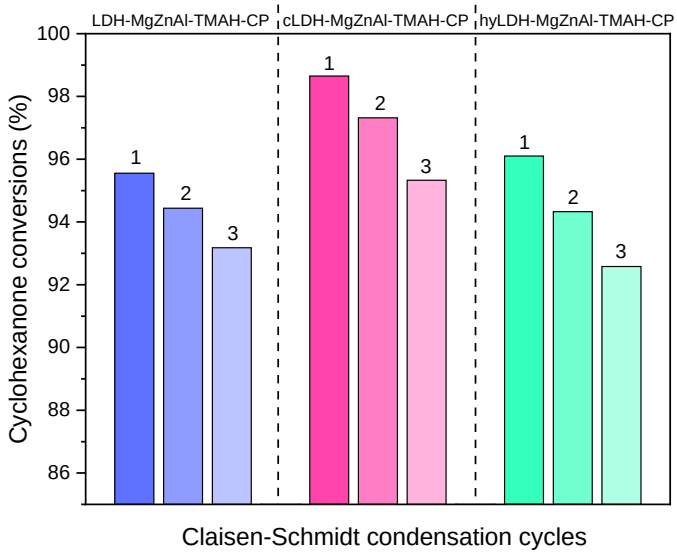

Figure 8. The catalyst reusability after 3 cycles in Claisen-Schmidt condensation for catalysts prepared by co-precipitation with organic alkalis.

3. Materials and Methods

3.1. Catalyst Preparation

The layered double hydroxide $Mg_{0.325}Zn_{0.325}Al_{0.25}$ was synthesized through both co-precipitation and mechano-chemical methods using the traditional inorganic alkalis but also a non-conventional organic base. Co-precipitation route with inorganic alkalis was carried out according to a methodology already reported [43], mixing solutions of $Mg(NO_3)_2{\cdot}6H_2O$, $Zn(NO_3)_2{\cdot}6H_2O$ and $Al(NO_3)_3{\cdot}9H_2O$ (0.325/0.325/0.25 molar ratio and 1.5M) in presence NaOH and Na_2CO_3 (NaOH / Na_2CO_3 of 2.5 molar ratio and 1M Na_2CO_3) at pH of 10, room temperature, 600 rpm. The TIM854, NB pH/EP/Stat pH-STAT Titrator was used to adding both solutions at a feed rate of 60 $mL{\cdot}h^{-1}$. The suspension was then aged for 18 h at 80 °C in air atmosphere, cooled at room temperature and filtered, washed with bi-distillated water until pH of 7 and dried for 24 h in air at 120 °C (**LDH-MgZnAl-CO_3^{2-}/OH^--CP**). After that, calcination of this sample at 460 °C for 18 h in air led to the corresponding mixed oxide (**cLDH-MgZnAl-CO_3^{2-}/OH^--CP**). The reconstruction of the layered structure was completed through memory effect by the immersion of cLDH-MgZnAl-CO_3^{2-}/OH^--CP in bi-distilled water for 24 h at room temperature, followed by drying for 24 h at 120 °C in air (**hyLDH-MgZnAl-CO_3^{2-}/OH^--CP**). The nontraditional mechano-chemical method was carried out by a direct milling of the precursors in a Mortar Grinder RM 200 for 1h at 100 rpm (**LDH-MgZnAl-CO_3^{2-}/OH^--MC**) at pH of approx. 10

Preprints (www.preprints.org) | NOT PEER-REVIEWED | Posted: 8 June 2022 doi:10.20944/preprints202206.0109.v1

with no water addition or additional aging process. Further protocols for mixed oxides and reconstructed layered samples were identical to the co-precipitation method (**cLDH-MgZnAl-CO_3^{2-}/OH^--MC** and **hyLDH-MgZnAl-CO_3^{2-}/OH^--MC**). Both co-precipitation and mechano-chemical routes were also used to generate LDH in the presence, of a non-traditional organic alkali represented by TMAH (TetraMethylAmonium Hydroxide; wt. 25% in water) maintaining the same operational parameters (**LDH-MgZnAl-TMAH-CP**; **cLDH-MgZnAl-TMAH-CP**; **hyLDH-MgZnAl-TMAH-CP**). Noteworthy, the bi-distilled water used in washing step was 10 times lower comparing to the case when inorganic alkalis were used as precipitation agent. A volume of TMAH identical to the one employed in the co-precipitation route was applied to obtain the LDH sample by mechano-chemical route (**LDH-MgZnAl-TMAH-MC**) under similar operating conditions (**cLDH-MgZnAl-TMAH-MC**; **hyLDH-MgZnAl-TMAH-MC**).

Index: LDH – layered double hydroxides; cLDH – mixed oxides; hyLDH – reconstructed layered structure; MgZnAl – the involved cations; CO_3^{2-}/OH^- - inorganic alkalis (Na_2CO_3/NaOH); TMAH – tetramethylammonium hydroxide; CP – co-precipitation; MC – mechano-chemical.

3.2. Catalyst Characterization

Powder X-ray diffraction patterns were recorded using a Shimadzu XRD 7000 diffractometer with Cu Kα radiation (λ = 1.5418 Å , 40 kV, 40 mA) at a scanning speed of 0.10°·min^{-1} in the 2θ range of 5 - 80°. DRIFTS spectra were recorded with JASCO FT/IR-4700 spectrometer by an accumulation of 128 scans in 400 - 4000 cm^{-1} domain. DR UV-VIS spectra were recorded in the range 900-200 nm on Jasco V-650 UV-VIS spectrophotometer with integration sphere using Spectralon as white reference. N_2 adsorption-desorption isotherms were determined using a Micromeritics ASAP 2010 instrument, where prior to nitrogen adsorption, samples were outgassed under vacuum for 24 h at 120 °C. The base character of the catalysts was determined by an irreversible adsorption of organic molecules of different *pKa* method [50-52] (*e.g.* acrylic acid, *pKa* = 4.2, for total base sites and phenol, *pKa* = 9.9, for strong base sites), where the number of weak and medium base sites was calculated as the difference between the amounts of adsorbed acrylic acid and phenol.

3.3. Catalytic tests

3.3.1. Claisen-Schmidt condensation

The Claisen-Schmidt condensation was carried out in a thermo-stated glass reactor provided with water cooled condenser, where a mixture of benzaldehyde (0.002 moles ReagentPlus >99%, Sigma-Aldrich), cyclohexanone (0.001 moles >99%, Sigma-Aldrich) and 20 mg of catalyst (at a benzaldehyde/catalyst ratio of 10/1) was stirred under solvent-free conditions for 2h at 120 °C [36]. After that the catalyst was removed by filtration, washed with 1 mL of toluene and the liquid mixture was analyzed by Thermo-Quest GC provided with FID detector and a capillary column of 30 m length with DB5 stationary phase. The compounds were identified by mass spectrometer coupled chromatography, using a GC/MS/MS Varian Saturn 2100 T equipped with a CP-SIL 8 CB Low Bleed/MS column of 30 m length and 0.25 mm diameter.

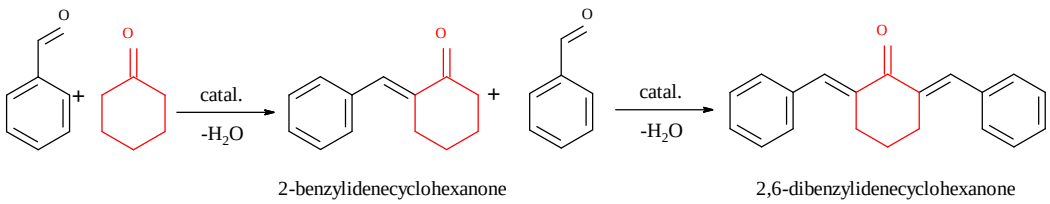

Scheme 1. Claisen-Schmidt condensation between benzaldehyde and cyclohexanone.

Preprints (www.preprints.org) | NOT PEER-REVIEWED | Posted: 8 June 2022 doi:10.20944/preprints202206.0109.v1

3.3.1. The aldol cyclohexanone self-condensation

The aldol cyclohexanone self-condensation was investigated in a similar reactor to the one utilized for the Claisen-Schmidt condensation mixing 0.01 moles of cyclohexanone with 5 %wt. catalyst under solvent-free conditions [53]. After 5h at reflux, the catalyst was removed from the mixture by filtration and the liquid reaction mixture was analyzed by GC-FID. Also, mass spectrometer coupled chromatography was used to compounds identification.

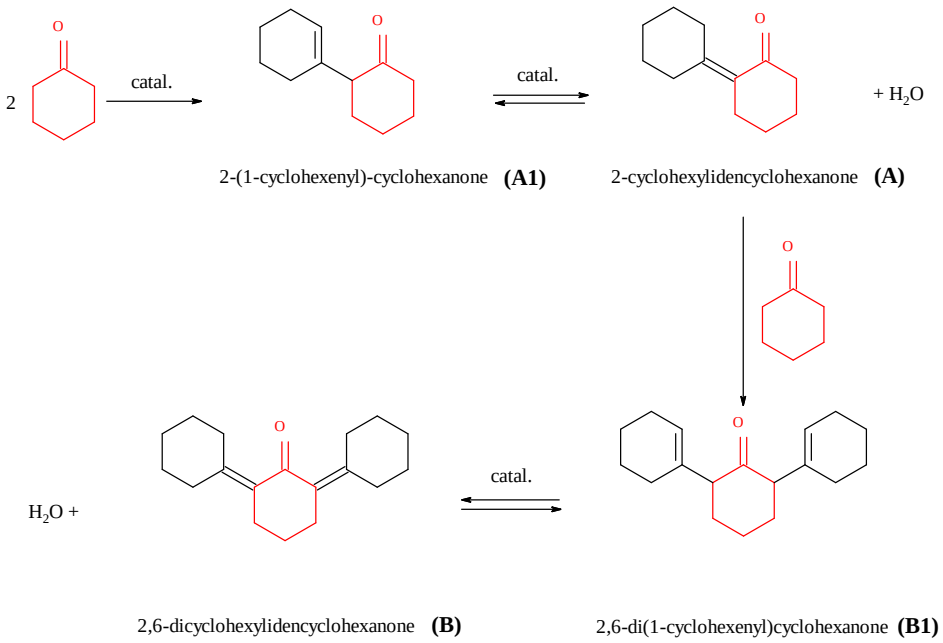

Scheme 2. The aldol self-condensation of cyclohexanone.

3.4. Catalyst Recycling

The LDH-MgZnAl-TMAH-CP, cLDH-MgZnAl-TMAH-CP and hyLDH-MgZnAl-TMAH-CP, the most active catalysts in their class, were selected for recycling tests. The layered catalysts were separated from the reaction mixture by filtration, washed with 1mL of toluene and dried for 5h at 120 °C in air before being used in the consecutive cycles. The same parameters were used for the mixed oxide with the specification that the thermal treatment was carried out at 460 °C.

4. Conclusions

Both preparation methods employed lead to the obtaining of LDH materials spiked with zincite phase. However, the amount of additional phase is higher in mechanochemically prepared catalysts. All solids exhibited the memory effect of the Mg/Al LDH phase while Zn was conserved as stable zincite phase. Using TMAH as organic alkali for LDH preparation brings the advantages of: *i)* a smaller quantity of water involved in the washing step, *ii)* preventing the contamination with alkali metal cations and *iii)* tailoring the LDH texture. Mechanochemically prepared materials show a pronounced basicity compared than that of the co-precipitated ones, while LDH materials prepared with TMAH present a higher basicity than that of LDH prepared with inorganic alkalis. Regardless of the preparation methods, organic/inorganic alkalis or reactions, the activity of catalysts decreased in the order: mixed oxides > reconstructed LDH > parent LDH samples. For Claisen-Schmidt condensation the conversions are higher than 90% after 2h with a total selectivity to 2,6-dibenzylidenecyclohexanone, while in self-condensation of cyclohexanone the conversion did not exceeded 7.29% after 5h. These catalytic behaviors are due to

Preprints (www.preprints.org) | NOT PEER-REVIEWED | Posted: 8 June 2022 doi:10.20944/preprints202206.0109.v1

the synergistic effect shown by the base sites as well as the pore size of the catalysts. The catalytic materials present a good stability after 3 cycles in Claisen-Schmidt condensation.

Supplementary Materials: Not applicable.

Author Contributions: Conceptualization, R.Z. and O.D.P.; methodology, S.D.M., B.C. and O.D.P.; investigation, R.Z., S.D.M., B.C., O.D.P.; resources, M.T. and E.E.J.; writing—original draft preparation, E.Z., O.D.P. and E.E.J.; writing—review and editing, V.I.P., O.D.P., S.O. and E.E.J.; supervision, R.Z., S.O. and V.I.P.; funding acquisition, M.S. and E.E.J.

All authors have read and agreed to the published version of the manuscript.

Funding: This work was financially supported by The Education, Scholarship, Apprenticeships and Youth Entrepreneurship Programmer – EEA Grants 2014-2021, Project No. 18-Cop-0041.

Data Availability Statement: The data are available on request from the corresponding author.

Conflicts of Interest: The authors declare no conflict of interest.

References

1. Basahel, S.N.; Al-Thabaiti, S.A.; Narasimharao, K.; Ahmed, N.S.; Mokhtar, M. Nanostructured Mg–Al Hydrotalcite as Catalyst for Fine Chemical Synthesis. *J. Nanosci. Nanotechnol*. **2014**, *14(2)*, 1931-1946. https://doi.org/10.1166/jnn.2014.9193
2. Wang, K.; Wang, T.; Islam, Q.A.; Wu, Y. Layered double hydroxide photocatalysts for solar fuel production. *Chinese J. Catal.* **2021**, *42*, 1944-1975. https://doi.org/10.1016/S1872-2067(21)63861-5
3. Yadav, G.D.; Wagh, Claisen-Schmidt Condensation using Green Catalytic Processes: A Critical Review. D.P. *ChemistrySelect* **2020**, *5(29)*, 9059-9085. https://doi.org/10.1002/slct.202001737
4. Cavani, F.; Trifiro, F.; Vaccari, A. Hydrotalcite-type anionic clays: Preparation, properties and applications. *Catal. Today* **1991**, *11*, 173-301. https://doi.org/10.1016/0920-5861(91)80068-K
5. Huang, Y.; Liu, C.; Rad, S.; He, H.; Qin, L. A Comprehensive Review of Layered Double Hydroxide-Based Carbon Composites as an Environmental Multifunctional Material for Wastewater Treatment. *Process.* **2022**, *10(4)*, 617. https://doi.org/10.3390/pr10040617
6. Johnston, A.-L.; Lester, E.; Williams, O.; Gomes, R.L. Understanding Layered Double Hydroxide properties as sorbent materials for removing organic pollutants from environmental waters. *J. Environ. Chem. Eng.* **2021**, *9(4)*, 105197. https://doi.org/10.1016/j.jece.2021.105197
7. Dias, A.C.; Ferreira Fontes, M.P. Arsenic (V) removal from water using hydrotalcites as adsorbents: A critical review. *Appl. Clay Sci*. **2020**, *191*, 105615. https://doi.org/10.1016/j.clay.2020.105615
8. Yang, H.; Xiong, C.; Liu, X.; Liu, A.; Li, T.; Ding, R.; Shah, S.P.; Li, W. Application of layered double hydroxides (LDHs) in corrosion resistance of reinforced concrete-state of the art. *Constr. Build. Mater.* **2021**, *307*, 124991. https://doi.org/10.1016/j.conbuildmat.2021.124991
9. Mohapi, M.; Sefadi, J.S.; Mochane, M.J.; Magagula, S.I.; Lebelo, K. Effect of LDHs and Other Clays on Polymer Composite in Adsorptive Removal of Contaminants: A Review. *Crystals* **2020**, *10(11)*, 957. https://doi.org/10.3390/cryst10110957
10. Ameena Shirin, V.K.; Sankar, R.; Johnson, A.P.; Gangadharappa, H.V.; Pramod, K. Advanced drug delivery applications of layered double hydroxide. *J. Control. Release* **2021**, *330*, 398-426. https://doi.org/10.1016/j.jconrel.2020.12.041
11. Lauermannová, A.-M.; Paterová, I.; Patera, J.; Skrbek, K.; Jankovský, O.; Bartůněk, V. Hydrotalcites in Construction Materials. *Appl. Sci*. **2020**, *10(22)*, 7989. https://doi.org/10.3390/app10227989
12. Ho, P.H.; Ambrosetti, M.; Groppi, G.; Tronconi, E.; Palkovits, R.; Fornasari, G.; Vaccari, A.; Benito, P. Structured Catalysts-Based on Open-Cell Metallic Foams for Energy and Environmental Applications. *Stud. Surf. Sci. Catal*. **2019**, *178*, 303-327. https://doi.org/10.1016/B978-0-444-64127-4.00015-X
13. Sikander, U.; Sufian, S.; Salam, M.A. A review of hydrotalcite based catalysts for hydrogen production systems. *Int. J. Hydrog. Energy* **2017**, *42*, 19851-19868. https://doi.org/10.1016/j.ijhydene.2017.06.089
14. Bravo-Suárez, J.J. Review of the synthesis of layered double hydroxides: a thermodynamic approach. *Quim. Nova* **2004**, *27*, 601-614. https://doi.org/10.1590/S0100-40422004000400015
15. Gonçalves, J.M.; Martins, P.R.; Angnes, L.; Araki, K. Recent advances in ternary layered double hydroxide electrocatalysts for the oxygen evolution reaction. *New J. Chem*. **2020**, *44*, 9981-9997. https://doi.org/10.1039/D0NJ00021C
16. Kühl, S.; Schumann, J.; Kasatkin, I.; Hävecker, M.; Schlögl, R.; Behrens, M. Ternary and quaternary Cr or Ga-containing ex-LDH catalysts—Influence of the additional oxides onto the microstructure and activity of $Cu/ZnAl_2O_4$ catalysts. *Catal. Today* **2015**, *246*, 92-100. https://doi.org/10.1016/j.cattod.2014.08.029
17. Ulibarri, M.A.; Pavlovic, I.; Barriga, C.; Hermosin, M.C.; Cornejo, Adsorption of anionic species on hydrotalcite-like compounds: effect of interlayer anion and crystallinity. *J. Appl. Clay Sci*. **2001**, *18*, 17-27. https://doi.org/10.1016/S0169-1317(00)00026-0
18. Takehira, K.; Shishido, T.; Shouro, D.; Murakami, K.; Honda, M.; Kawabata, T.; Takaki, K. Novel and effective surface enrichment of active species in Ni-loaded catalyst prepared from Mg–Al hydrotalcite-type anionic clay. *Appl. Catal. A: Gen.* **2005**, *279*, 41-51. https://doi.org/10.1016/j.apcata.2004.10.010

Preprints (www.preprints.org) | NOT PEER-REVIEWED | Posted: 8 June 2022 doi:10.20944/preprints202206.0109.v1

19. Marchi, A.J.; Apesteguia, C.R. Impregnation-induced memory effect of thermally activated layered double hydroxides. *Appl. Clay Sci*. **1998**, *13*, 35-48. https://doi.org/10.1016/S0169-1317(98)00011-8
20. Teodorescu, F.; Paladuta, A.-M.; Pavel, O.D. Memory effect of hydrotalcites and its impact on cyanoethylation reaction. *Mater. Res. Bull*. **2013**, *48*, 2055-2059. https://doi.org/10.1016/j.materresbull.2013.02.018
21. Barbosa, C.A.S.; A Ferreira,.M.D.C.; Constantino, V.R.L.; Coelho, A.C.V. Preparation and Characterization of Cu(II) Phthalocyanine Tetrasulfonate Intercalated and Supported on Layered Double Hydroxides. *J. Incl. Phenom*. **2002**, *42*, 15-23. https://doi.org/10.1023/A:1014598231722
22. He, J.; Wei, M.; Li, B.; Kang, Y.; Evans, D.G.; Duan, X. Preparation of Layered Double Hydroxides. *Struct. Bond*. **2006**, *119*, 89-119. https://doi.org/10.1007/430_006
23. Pavel, O.D.; Stamate, A.-E.; Zăvoianu, R.; Bucur, I.C.; Bîrjega, R.; Angelescu, E.; Pârvulescu, V.I. Mechano-chemical versus co-precipitation for the preparation of Y-modified LDHs for cyclohexene oxidation and Claisen-Schmidt condensations. *Appl. Catal. A Gen*. **2020**, *605*, 117797. https://doi.org/10.1016/j.apcata.2020.117797
24. Chen, L.J.; Sun, B.; Wang, X.D.; Qiao, F.M.; Ai, S.Y. 2D ultrathin nanosheets of Co–Al layered double hydroxides prepared in l-asparagine solution: enhanced peroxidase-like activity and colorimetric detection of glucose. *J. Mater. Chem. B* **2013**, *1*, 2268-2274. https://doi.org/10.1039/C3TB00044C
25. Wang, Y.Y.; Zhang, Y.Q.; Liu, Z.J.; Xie, C.; Feng, S.; Liu, D.D.; Shao, M.F.; Wang, S.Y. Layered Double Hydroxide Nanosheets with Multiple Vacancies Obtained by Dry Exfoliation as Highly Efficient Oxygen Evolution Electrocatalysts. *Angew. Chem., Int. Ed*. **2017**, *56*, 5867-5871. https://doi.org/10.1002/anie.201701477
26. Musella, E.; Gualandi, I.; Scavetta, E.; Rivalta, A.; Venuti, E.; Christian, M.; Morandi, V.; Mullaliu, A.; Giorgetti, M.; Tonelli, D. Newly developed electrochemical synthesis of Co-based layered double hydroxides: toward noble metal-free electro-catalysis. *J. Mater. Chem. A* **2019**, *7*, 11241-11249. https://doi.org/10.1039/C8TA11812D
27. Rong, F.; Zhao, J.; Yang, Q.; Li, C. Nanostructured hybrid NiFeOOH/CNT electrocatalysts for oxygen evolution reaction with low overpotential. *RSC Adv*. **2016**, *6*, 74536-74544. https://doi.org/10.1039/C6RA16450A
28. Ciotta, E.; Pizzoferrato, R.; Di Vona, M.L.; Ferrari, I.V.; Richetta, M.; Varone, A. Increasing the Electrical Conductivity of Layered Double Hydroxides by Intercalation of Ionic Liquids. *Mater. Sci. Forum* **2018**, *941*, 2209-2213. https://doi.org/10.4028/www.scientific.net/MSF.941.2209
29. Pavel, O.D.; Stamate, A.-E.; Bacalum, E.; Cojocaru, B.; Zăvoianu, R.; Pârvulescu, V.I. Catalytic behavior of Li-Al-LDH prepared via mechanochemical and co-precipitation routes for cyanoethylation reaction, *Catal. Today* **2021**, *366*, 227-234. https://doi.org/10.1016/j.cattod.2020.06.019
30. Schmidt, J.G. Ueber die Einwirkung von Aldehyd auf Furfurol. *Ber. Dtsch. Chem. Ges*. **1880**, *13*, 2342-2345. https://doi.org/10.1002/cber.188001302266
31. Claisen, L. Condensationen der Aldehyde mit Acetessig- und Malonsäureäther. *Ber. Dtsch. Chem. Ges*. 1881, *14*, 345-349. https://doi.org/10.1002/cber.18810140181
32. Sallum, L.O.; Duarte, V.S.; Custodio, J.M.F.; Faria, E.C.M.; da Silva, A.M.; Lima, R.S.; Camargo, A.J.; Napolitano, H.B. Cyclohexanone-Based Chalcones as Alternatives for Fuel Additives. *ACS Omega* **2022**, *7(14)*, 11871-11886. https://doi.org/10.1021/acsomega.1c07333
33. Eagon, S.; Hammill, J.T.; Fitzsimmons, K.; Sienko, N.; Nguyen, B.; Law, J.; Manjunath, A.; Wilkinson, S.P.; Thompson, K.; Glidden, J.E.; Rice, A.L.; Falade, M.O.; Kimball, J.J.; Di Bernardo, C.; R. Guy K. Antimalarial activity of 2,6-dibenzylidenecyclohexanone derivatives. *Bioorg. Med. Chem. Lett*. **2021**, *47*, 128216. https://doi.org/10.1016/j.bmcl.2021.128216
34. Tang, Y.; Xu, J.; Gu, X. Modified calcium oxide as stable solid base catalyst for Aldol condensation reaction. *J. Chem. Sci*. **2013**, *125*, 313-320. https://doi.org/10.1007/s12039-013-0362-5
35. Sluban, M.; Cojocaru, B.; Parvulescu, V.I.; Iskra, J.; Korošec, R.C.; P Umek. Protonated titanate nanotubes as solid acid catalyst for aldol condensation. *J. Catal*. **2017**, *346*, 161-169. https://doi.org/10.1016/j.jcat.2016.12.015
36. Jain, D.; Khatri, C.; Rani, A. Synthesis and characterization of novel solid base catalyst from fly ash. *Fuel* **2011**, *90(6)*, 2083-2088. https://doi.org/10.1016/j.fuel.2010.09.025
37. Motiur Rahman, A.F.M.; Ali, R.; Jahng, Y.; Kadi, A.A. A Facile Solvent Free Claisen-Schmidt Reaction: Synthesis of α,α'-bis-(Substituted-benzylidene)cycloalkanones and α,α'-bis-(Substituted-alkylidene)cycloalkanones. *Molecules* **2012**, *17(1)*, 571-583. https://doi.org/10.3390/molecules17010571
38. Mortezaei, Z.; Zendehdel, M.; Bodaghifard, M.A. Synthesis and characterization of functionalized NaP Zeolite@$CoFe_2O_4$ hybrid materials: a micro–meso-structure catalyst for aldol condensation. *Res Chem Intermed* **2020**, *46*, 2169-2193. https://doi-org.am.e-nformation.ro/10.1007/s11164-020-04085-z
39. Vashishtha, M.; Mishra, M.; Undre, S.; Singh, M.; Shah, D.O. Molecular mechanism of micellar catalysis of cross aldol reaction: Effect of surfactant chain length and surfactant concentration. *J. Mol. Catal. A Chem*. **2015**, *396*, 143-154. https://doi.org/10.1016/j.molcata.2014.09.023
40. Hu, Z.G.; Liu, J.; Zeng, P.L.;Dong, Z.B. Synthesis of α, α'-bis(substituted benzylidene)ketones catalysed by a $SOCl_2$/EtOH reagent. *J. Chem. Res*. **2004**, *1*, 55-56. https://doi.org/10.3184/030823404323000792
41. Miyata, S. The Syntheses of Hydrotalcite-Like Compounds and Their Structures and Physico-Chemical Properties—I: the Systems Mg^{2+}-Al^{3+}-NO^-_3, Mg^{2+}-Al^{3+}-Cl^-, Mg^{2+}-Al^{3+}-ClO^-_4, Ni^{2+}-Al^{3+}-Cl^- and Zn^{2+}-Al^{3+}-Cl^-. *Clays Clay Miner*. **1975**, *23*, 369–375. https://doi.org/10.1346/CCMN.1975.0230508

Preprints (www.preprints.org) | NOT PEER-REVIEWED | Posted: 8 June 2022 doi:10.20944/preprints202206.0109.v1

42. Musker, W.K. A Reinvestigation of the Pyrolysis of Tetramethylammonium Hydroxide. *J. Am. Chem. Soc*. **1964**, *86*(5), 960–961. https://doi.org/10.1021/ja01059a070
43. Pavel, O.D.; Zăvoianu, R.; Bîrjega, R.; Angelescu, E.; Pârvulescu, V.I. Mechanochemical versus co-precipitated synthesized lanthanum-doped layered materials for olefin oxidation. *Appl Catal A Gen.* **2017**, *542*, 10-20. https://doi.org/10.1016/j.apcata.2017.05.012
44. Frost, R.L.; Cash, G.A.; Kloprogge, J.T. `Rocky Mountain leather', sepiolite and attapulgite—an infrared emission spectroscopic study. *Vib. Spectrosc*. **1998**, *16*, 173-184. https://doi.org/10.1016/S0924-2031(98)00014-9
45. Singh, D.K.; Pandey, D.K.; Yadav, R.R.; Singh, D. A study of nanosized zinc oxide and its nanofluid. *Pramana* **2012**, *78(5)*, 759-766. https://www.ias.ac.in/article/fulltext/pram/078/05/0759-0766
46. Anandan, K.; Siva, D.; Rajesh, K. Structural and optical properties of (ZnO/MgO) nanocomposites. *Int. J. Eng. Res. Technol*. **2018**, *7(8)*, 493-499. DOI: 10.5281/zenodo.1401731
47. Yousefi, S.; Ghasemi, B.; Tajally, M.; Asghari, A. Optical properties of MgO and $Mg(OH)_2$ nanostructures synthesized by a chemical precipitation method using impure brine. *J. Alloys Compd.* **2017**, *711*, 521-529. https://doi.org/10.1016/j.jallcom.2017.04.036
48. Winter, F.W.; Xia, X.; Hereijgers, B.P.C.; Bitter, J.H.; van Dillen, A.J.; Muhler, M.; de Jong, K.P. On the Nature and Accessibility of the Brønsted-Base Sites in Activated Hydrotalcite Catalysts. *J. Phys. Chem. B* **2006**, *110(18)*, 9211–9218. https://doi.org/10.1021/jp0570871
49. Pavel, O.D.; Bîrjega, R.; Che, M.; Costentin, G.; Angelescu, E.; Şerban, S. The activity of Mg/Al reconstructed hydrotalcites by "memory effect" in the cyanoethylation reaction. *Catal. Commun*. **2008**, *9*, 1974-1978. https://doi.org/10.1016/j.catcom.2008.03.027
50. Debecker, D.P.; Gaigneaux, E.M.; Busca, G. Exploring, Tuning, and Exploiting the Basicity of Hydrotalcites for Applications in Heterogeneous Catalysis. *Chem.-Eur. J.* **2009**, *15*, 3920-3935. https://doi.org/10.1002/chem.200900060
51. Parida, K.; Das, Mg/Al hydrotalcites: preparation, characterisation and ketonisation of acetic acid. J. *J. Mol. Catal. A-Chem*. **2000**, *151*, 185-192. https://doi.org/10.1016/S1381-1169(99)00240-X
52. O.D. Pavel, R. Zăvoianu, R. Bîrjega, E. Angelescu, The effect of ageing step elimination on the memory effect presented by $Mg_{0.75}Al_{0.25}$ hydrotalcites (HT) and their catalytic activity for cyanoethylation reaction. *Catal. Commun*. **2011**, *12*, 845-850. https://doi.org/10.1016/j.catcom.2011.02.005
53. Angelescu, E.; Birjega, R.; Pavel, O.D.; Che, M.; Costentin, G.; Popoiu; S. Hydrotalcites (HTs) and mesoporous mixed oxides obtained from HTs, basic solid catalysts for cyclohexanone condensation. *Stud. Surf. Sci. Catal*. **2005**, *156*, 257-264. https://doi.org/10.1016/S0167-2991(05)80216-2